Available online at www.sciencedirect.com
SCIENCE DIRECT®

JOURNAL OF COMPUTATIONAL AND APPLIED MATHEMATICS

ELSEVIER Journal of Computational and Applied Mathematics 168 (2004) 21–29

www.elsevier.com/locate/cam

Electromagnetic analysis of horizontal wire in two-layered soil

Vesna Arnautovski-Toseva*, Leonid Grcev

Faculty of Electrical Engineering, University "SS Cyril & Methodus", Skopje, Macedonia

Received 27 September 2002; received in revised form 31 May 2003

Abstract

Simulation of grounding systems at high frequencies is of interest in electromagnetic compatibility, especially related to lightning, and in emerging technologies, such as power line telecommunications. This paper presents first results in the effort to extend the electromagnetic field theory based modeling of grounding systems to a two-layer model of earth. A rigorous mathematical model which solution involves numerical solution of Sommerfeld-type integrals is described. Also new more approximate but computationally more efficient solution based on quasi-static image theory is introduced. Comparison between these two solutions led to conclusion related to the applicability of the image theory approach, which may be of interest for practical problems.

Keywords: Modeling; Grounding electrodes; Transient analysis; Frequency domain analysis; Two-layered soil; Integral equations; Green's functions

1. Introduction

Simulation of grounding systems at high frequencies is of interest in electromagnetic compatibility studies, especially in relation to lightning [17]. Grounding systems are usually modeled by a circuit theory approach, based on quasi-static approximation [14], which imposes limit of application to lower frequencies, typically below 1 MHz [16,13]. Since many lightning related studies require analysis in frequency ranges up to few MHz, and some emerging technologies, such as power line communications, up to few tens of MHz [18], there is a need for more accurate modeling in MHz range. Grounding systems and connected structures often obey thin wire approximation, which enables efficient use of method of moment computational techniques [10]. Application of these powerful modeling methods led to the most accurate modeling of grounding systems at high frequencies [7–9]. A special problem in modeling of grounding systems is modeling of the surrounding soil.

* Corresponding author.
E-mail address: atvesna@etf.ukim.edu.mk (V. Arnautovski-Toseva).

0377-0427/$ - see front matter
doi:10.1016/j.cam.2003.05.014

Although the earth is inherently nonhomogeneous it is often represented by a homogeneous model with some estimated apparent constants of resistivity and permittivity (permeability of air is usually applied) [15]. However, recently methods for estimating an equivalent two-layer earth models have been established [4] leading to significant advancement in grounding systems modeling [19]. So far this advancement in the modeling was limited to the low-frequency case.

This paper presents first results in the effort to extend the electromagnetic field theory based modeling of grounding systems to a two-layer model of earth. Furthermore, since the solution of the exact mathematical model involve intense computations that usually require large computer resources, this solution is compared with a more approximate but more computationally efficient solution, based on the image theory, that may be of more interest in practical applications. In relation to this, new formula for application of quasi-static image theory in grounding system analysis is introduced. Analysis in this paper is limited to horizontal grounding electrodes.

2. The mathematical model of the grounding system

The electromagnetic full-wave model developed for analysis of grounding systems in homogeneous earth [7–9] was based on rigorous formulations derived from the full set of the Maxwell's equations, on the theoretical background of antenna analysis [3]. The solution was based on the exact solution of fields due to electrical dipole in or near lossy half-space [1]. We follow the similar idea to extend the analysis to two-layer earth model. We apply the exact model for layered media developed in antenna theory [11,12,5]. Here, for completeness, only short account of the development of the mathematical model is given, while the important modifications of the solution of the mathematical model, required for grounding system analysis, are given in Section 3.

The model is based on the following assumptions: (1) The earth and the air occupy half-spaces with a common horizontal plane boundary between them, where the earth consists of two layers one with finite and the other with infinite depth separated with a plane boundary parallel to the earth–air interface. (2) The earth and the grounding electrodes exhibit linear and isotropic characteristics: conductivity, permittivity and permeability. (3) The grounding system is modeled as network of horizontal cylindrical metallic conductors, which are assumed to be subject to the thin-wire approximation, i.e., the ratio of the length of the conductor segment to its radius is $\gg 1$. (4) The energizing of the grounding system is by injection of current at an end point of one of the conductors.

An idealized two-layered soil model, which is used for this theoretical development, is shown in Fig. 1. It consists of an upper layer (medium 1) of finite depth d_1 which is characterized by relative permittivity ε_{r1}, permeability μ_0 and conductivity σ_1; and a lower layer of infinite depth (medium 2) which is characterized by relative permittivity ε_{r2}, permeability μ_0 and conductivity σ_2. The air (medium 3) is characterized by permittivity ε_0, permeability μ_0 and zero conductivity.

We use the mixed-potential integral equation (MPIE) [11] as a basis of the mathematical model. Based on usual method of moment techniques, we consider the grounding system divided in a number of fictitious segments. A point at the source segment is defined by a vector $\vec{r'} = (x', y', z')$, and the position of the observer (testing) segment is defined by a vector $\vec{r} = (x, y, z)$ (both segments are arbitrarily positioned on the $x - y$ plane). In MPIE formulation, the electric field vector $\vec{E}(\vec{r})$ is expressed in terms of magnetic vector potential $\vec{A}(\vec{r})$ and electric scalar potential $\phi(\vec{r})$, due to

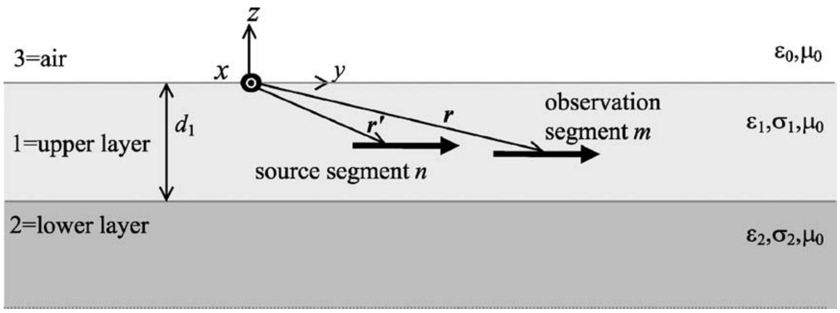

Fig. 1. A two-layer soil model and the coordinate system used in the analysis.

current $I(\vec{r'})$ and charge $q(\vec{r'})$ along the source segment axis ℓ_n, respectively:

$$\vec{E}(\vec{r}) = -\nabla\phi(\vec{r}) - \jmath\omega\vec{A}(\vec{r}) \tag{1}$$

which could be represented in integral form by

$$\phi(\vec{r}) = \int_{\ell_n} G_\phi(\vec{r}|\vec{r'})q(\vec{r'})\,\mathrm{d}\ell', \quad \vec{A}(\vec{r}) = \int_{\ell_n} \underline{\mathbf{G}}_A(\vec{r}|\vec{r'})\cdot\vec{I}(\vec{r'})\,\mathrm{d}\ell'. \tag{2}$$

Here, $\underline{\mathbf{G}}_A$ is dyadic Green's function of the magnetic vector potential and G_ϕ is the scalar potential Green's function. The expressions for the Green's functions due to a horizontal electric dipole in the upper layer are adequately derived in the spectral domain firstly following the general form of the spectral domain Green's functions for microstrip geometry [5] used in the analysis of printed antennas. The spectral domain Green's functions for the source in the upper layer show the z-dependence of the fields in the source region, which can be written as a sum of the direct term and up- and down-going waves due to reflections from the interfaces $z=-d_1$ and 0, respectively:

$$\tilde{G}^A_{xx} = \mu_0\left[\tilde{G}_{\mathrm{dir}} + \frac{A_\mathrm{h}\mathrm{e}^{\mathrm{j}k_{z1}(z-z')}}{\mathrm{j}k_{z1}} + \frac{C_\mathrm{h}\mathrm{e}^{-\mathrm{j}k_{z1}(z-z')}}{\mathrm{j}k_{z1}}\right], \tag{3}$$

$$\tilde{G}^A_{zx} = \mathrm{j}\mu_0\left[\frac{k_x}{k_\rho^2}(A_\mathrm{h}+B_\mathrm{h})\mathrm{e}^{\mathrm{j}k_{z1}(z-z')} + \frac{k_x}{k_\rho^2}(D_\mathrm{h}-C_\mathrm{h})\mathrm{e}^{-\mathrm{j}k_{z1}(z-z')}\right], \tag{4}$$

$$\tilde{G}_\phi = \frac{1}{n_1^2}\left[\tilde{G}_{\mathrm{dir}} + \frac{k_{z1}^2B_\mathrm{h}+k_1^2A_\mathrm{h}}{k_\rho^2\mathrm{j}k_{z1}}\,\mathrm{e}^{\mathrm{j}k_{z1}(z-z')} + \frac{k_1^2C_\mathrm{h}-k_{z1}^2D_\mathrm{h}}{k_\rho^2\mathrm{j}k_{z1}}\,\mathrm{e}^{-\mathrm{j}k_{z1}(z-z')}\right], \tag{5}$$

where, $\tilde{G}_{\mathrm{dir}}=\mathrm{e}^{-\mathrm{j}k_{z1}|z+z'|}/\mathrm{j}k_{z1}$, where $n_1^2=\varepsilon_{r1}-\mathrm{j}\sigma_1/(\omega\varepsilon_0)$ and $n_2^2=\varepsilon_{r2}-\mathrm{j}\sigma_2/(\omega\varepsilon_0)$ are complex dielectric constants of the ground layers, and $k_i^2=\omega^2\mu_0n_i^2$ are propagation constants. The up- and down-going waves are represented by terms A_h, B_h, C_h and D_h:

$$A_\mathrm{h} = \frac{\mathrm{e}^{-\mathrm{j}k_{z1}|z'|}R^{10}_{\mathrm{TE}}\left[\mathrm{e}^{-\mathrm{j}k_{z1}|z'|)} + R^{12}_{\mathrm{TE}}\mathrm{e}^{-\mathrm{j}k_{z1}(2d_1-|z'|)}\right]}{1-R^{12}_{\mathrm{TE}}R^{10}_{\mathrm{TE}}\mathrm{e}^{-\mathrm{j}k_{z1}2d_1}}, \tag{6}$$

$$B_{\mathrm{h}} = \frac{\mathrm{e}^{-\mathrm{j}k_{z1}|z'|} R_{\mathrm{TM}}^{10} \left[\mathrm{e}^{-\mathrm{j}k_{z1}|z'|)} - R_{\mathrm{TM}}^{12} \mathrm{e}^{-\mathrm{j}k_{z1}(2d_1-|z'|)}\right]}{1 - R_{\mathrm{TM}}^{12} R_{\mathrm{TM}}^{10} \mathrm{e}^{-\mathrm{j}k_{z1}2d_1}}, \tag{7}$$

$$C_{\mathrm{h}} = \frac{\mathrm{e}^{-\mathrm{j}k_{z1}(d_1-|z'|)} R_{\mathrm{TE}}^{12} \left[\mathrm{e}^{-\mathrm{j}k_{z1}(d_1-|z'|)} + R_{\mathrm{TE}}^{10} \mathrm{e}^{-\mathrm{j}k_{z1}(d+|z'|)}\right]}{1 - R_{\mathrm{TE}}^{12} R_{\mathrm{TE}}^{10} \mathrm{e}^{-\mathrm{j}k_{z1}2d_1}}, \tag{8}$$

$$D_{\mathrm{h}} = \frac{\mathrm{e}^{-\mathrm{j}k_{z1}(d_1-|z'|)} R_{\mathrm{TM}}^{12} \left[-\mathrm{e}^{-\mathrm{j}k_{z1}(d_1-|z'|)} + R_{\mathrm{TM}}^{10} \mathrm{e}^{-\mathrm{j}k_{z1}(d_1+|z'|)}\right]}{1 - R_{\mathrm{TM}}^{12} R_{\mathrm{TM}}^{10} \mathrm{e}^{-\mathrm{j}k_{z1}2d_1}} \tag{9}$$

which are functions of generalized reflection coefficients R_{TM} and R_{TE}

$$R_{\mathrm{TE}}^{10} = \frac{k_{z1} - k_{z0}}{k_{z1} + k_{z0}}, \quad R_{\mathrm{TE}}^{12} = \frac{k_{z1} - k_{z2}}{k_{z1} + k_{z2}}, \tag{10}$$

$$R_{\mathrm{TM}}^{10} = \frac{k_{z1} - n_1^2 k_{z0}}{k_{z1} + n_1^2 k_{z0}}, \quad R_{\mathrm{TM}}^{12} = \frac{n_2^2 k_{z1} - n_1^2 k_{z2}}{n_2^2 k_{z1} + n_1^2 k_{z2}} \tag{11}$$

with $k_{zi}^2 = k_i^2 - k_\rho^2$ for $i = 0, 1, 2$; $k_\rho^2 = k_x^2 + k_y^2$. The spatial domain Green's functions are obtained by solving Sommerfeld integrals of the following type which are integrated numerically:

$$G_{A,\phi} = \frac{1}{4\pi} \int_0^\infty \tilde{G}_{A,\phi}(k_\rho) J_0(k_\rho \rho) k_\rho \, \mathrm{d}k_\rho. \tag{12}$$

3. Solution of the mathematical model of the grounding system

Since the mathematical model described in Section 2 was originally developed in antenna theory, a number of modifications and extensions are necessary for its application in grounding systems analysis. The details of the modifications may be found in [6] and validation by comparison with field experiments in [7]. Here only short account of the main differences with antenna theory is given: the definition of the source, evaluation of the impedance to ground, and computational effort for direct numerical solution of the Sommerfed-type integrals. The main difference with the antenna theory regards the definition of the source. In antenna theory usually the voltage source between two closely positioned terminals is defined. In grounding system analysis, the injected current is usually known and the property that characterizes the grounding system behavior is the impedance to ground. It is defined as a ratio of the voltage between the feed point at the grounding system to a point at remote neutral ground along a given path. Fig. 2 illustrates the applied solution. The source is modeled by an ideal current source connected with the one terminal to the end point of a grounding electrode and with the other to the ground at infinity, while the influence of connecting leads is neglected. We have applied the Galerkin solution [10] with triangular basis and test functions, in which the derivatives of the scalar potential are in effect replaced by finite differences. Therefore, the current injection is modeled by an additional ‘triangle’ at the point of injection. The current distribution is computed as a response to an injected current I_{S}, as a solution of the following form

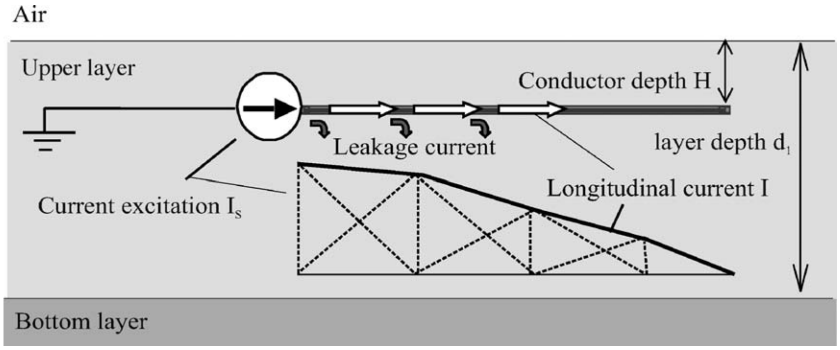

Fig. 2. A general view of an end-driven single grounding conductor with longitudinal current approximated by triangle functions.

of the matrix equation:

$$[Z][I] = [Z' I_S], \tag{13}$$

where the column matrix $[I]$ represents the unknown currents to be determined, $[Z]$ is the matrix of mutual impedances between each of current elements, $[Z' I_S]$ is energization matrix related to the energizating by injection of current I_S, and Z' is impedance matrix between the segment where the currents are injected and the other segments. Once the current distribution along the conductors is computed, the electric field at points of given profiles can be computed by summing the contributions due to currents in each segment. To compute the voltage between the feed point and a remote point in earth V_S, a profile starting from the surface of the conductor is used. This leads to the impedance to ground formulation by

$$Z_S = \frac{V_S}{I_S} = \frac{1}{I_S}[I] \cdot [Z_S] = [Z]^{-1} \cdot [Z'] \cdot [Z_S], \tag{14}$$

where $[Z_S]$ is the impedance matrix between segments and injection segment.

3.1. *Specifics concerning numerical solution of Sommerfeld-type integrals in grounding system analysis*

In the field of microwave technology the spectrum of interest is of the order GHz. The calculation domain of interest covers the range of the far fields where the saddle-point method is found to be adequate procedure for calculation of (12). For the near-field calculation generally it is possible to perform analytical or approximation integration by the following simplification $k_{z1}^2 \approx k_{z0}^2$ since layers are generally loss-less. However in the grounding system studies the frequency domain analysis of the response to a typical lightning current impulses has to cover the frequency spectrum from 100 Hz to 100 MHz. Considering the geometry of the grounding conductors (several hundreds m), the distance between source and observation point varies from dimensions much smaller than the wavelength to several times of the order of the wavelength, which covers the near field to intermediate field zone. For adequate procedure for solving (12) the detailed analysis of the analytical properties of integrands is necessary. For very small distance between source and observation point (near-field range ($k_0\rho < 1 < k_1\rho$) it appeared that quasi-static method of images is adequately applicable. The exact numerical integration procedure of (12) is appropriate in the cases when the distance between source and observation point is of the order of the wavelength. The resistivity of ground varies from 10 Ωm that represents the ground as highly conductive medium, to several 10 000 Ωm. The parameters of the two-layer ground which are represented by the frequency-dependent complex constants n_1^2 and n_2^2, in the low-frequency spectrum in highly conductive soil layers are characterized by a very large imaginary part. It is often found that direct numerical evaluation of the integrals is numerically unstable and extremely computer time consuming. Our tests of the CPU time needed for calculation of Sommerfeld integrals have suggested that it is significantely increased in case of high conductivity of the layers.

3.2. *Quasi-static image model*

Looking for computationally more efficient solution we compare the above described method with the quasi-static method of images. It is defined for the scalar potential due to point current source and its multiple images of decreasing strength. Our approach is based on [2], where the scalar potential Green's function in the upper layer of two-layered soil is written in the following infinite summation term

$$G_\phi = \sum_{i=0}^{\infty} (V_1 V_2)^i \left[\frac{e^{-jk_1 R_{i1}}}{R_{i1}} + V_1 \frac{e^{-jk_1 R_{i2}}}{R_{i2}} + V_2 \frac{e^{-jk_1 R_{i3}}}{R_{i3}} + V_1 V_2 \frac{e^{-jk_1 R_{i4}}}{R_{i4}} \right], \tag{15}$$

where R_{ij}, $j = 1, \ldots, 4$ are distances from source and source images to the observation point, and V_1 and V_2 are reflection coefficients at the lower and upper boundary, respectively [2].

4. Numerical results

As an illustrative example, we consider a two-layer soil which is characterized by relative permittivity $\varepsilon_{r1,r2} = 10$, and its upper layer conductivity $\sigma_1 = 0.01$ S/m, and the bottom layer conductivity: (1) $\sigma_2 = 0.000526$ S/m, with reflection factor $K = +0.9$, or (2) $\sigma_2 = 0.19$ S/m, with reflection factor $K = -0.9$, where $K = (\sigma_1 - \sigma_2)/(\sigma_1 + \sigma_2)$. It is assumed that the upper layer height varies form: $d_1 = 1.2$, 2.0 and 5.0 m. The studied conductor is 100 m typical horizontal linear end-driven grounding electrode with diameter of 10 cm placed at $H = 1$ m depth. It is energized by a time-harmonic current generator with amplitude of 1 A.

Fig. 3 shows the longitudinal current profiles (real and imaginary parts) when the reflection factor is $K = +0.9$ and -0.9 for frequencies: (a) 1 kHz (wavelength in the upper layer $\lambda_1 \approx 710$ m), (b) 10 kHz ($\lambda_1 \approx 224$ m), (c) 0.1 MHz ($\lambda_1 \approx 71$ m) and (d) 1.0 MHz ($\lambda_1 \approx 22$ m). It is shown that the performance of a 100 m horizontal grounding electrode placed in two-layer soil is not only function of frequency, but is significantly influenced by the reflection factor K and the upper layer depth d_1. It is observed that up to 1 kHz the longitudinal current distribution profiles correspond to the typical quasi-static profiles. Significant differences are observed for frequencies from 10 kHz up to several 100 kHz. As the frequency increases, it is observed that a larger part of the injected current is discharged through a smaller section at the beginning of a conductor. This tendency is emphasized

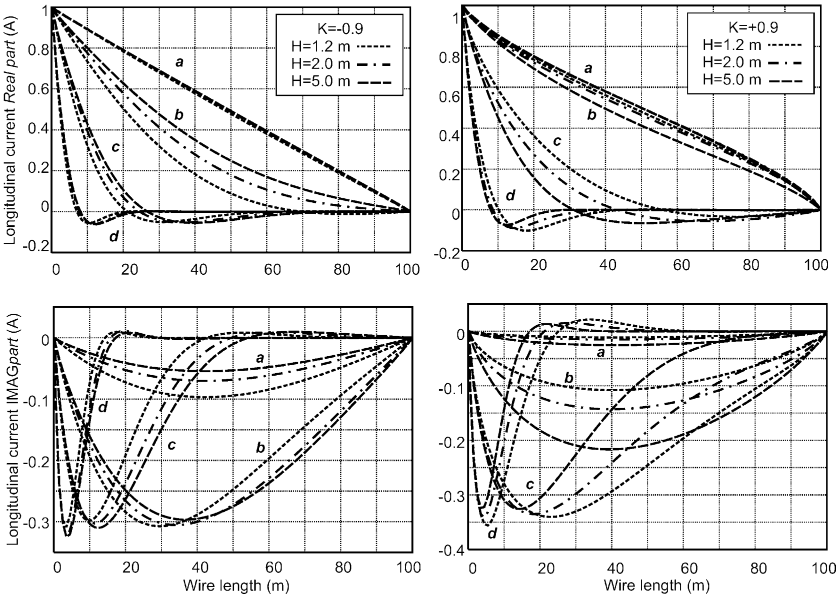

Fig. 3. Current distribution along a studied 100 m horizontal grounding conductor.

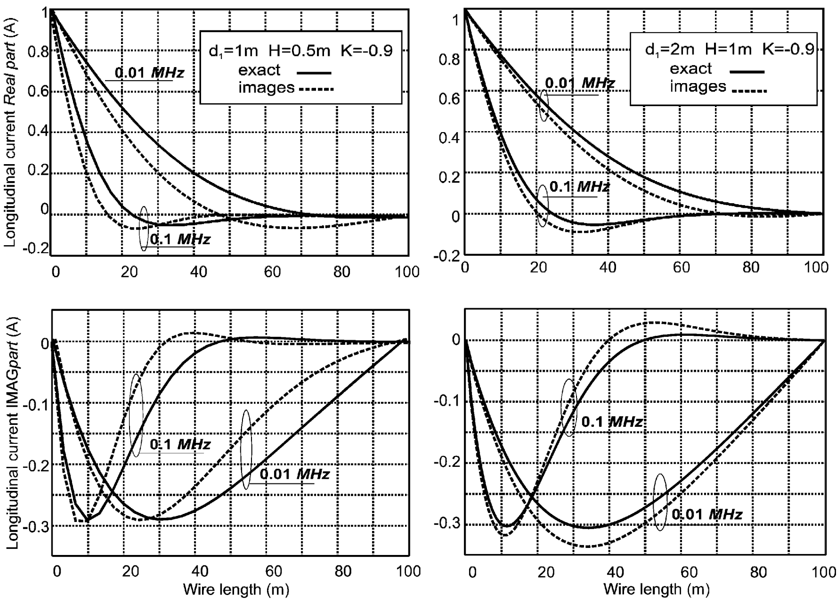

Fig. 4. Comparison between exact and image model regarding longitudinal current along a 100 m horizontal grounding conductor with respect to layer depth.

when the lower layer is much more conductive than the upper layer, especially when $d_1 = 1.2$ m. At frequencies over 1 MHz the current distribution profiles are slightly influenced by the parameters of a two-layer structure and approaches that of a uniform soil.

Fig. 4 shows the comparative results of the longitudinal current along 100 m conductor when $K = -0.9$ calculated by the exact model and quasi-static image method. The studied frequencies are 0.01 and 0.1 MHz. The studied cases are: (1) upper layer depth $d_1 = 2$ m and wire depth $H = 1$ m; and (2) upper layer depth $d_1 = 1$ m and wire depth $H = 0.5$ m. The results show that the image model gives acceptable results whenever the upper layer depth is large. However significant differences between the exact approach and the method of images are observed when the upper layer depth is thin.

5. Conclusion

This paper describes the mathematical model and its computational solution for an electromagnetic analysis of grounding systems in two-layer soil. Also, new more approximate but more computationally efficient solution is introduced by application of quasi-static image theory. The preliminary results led to the following conclusions: (1) High-frequency behavior of horizontal conductors in two-layer soil is significantly affected by the parameters of both layers, especially when the upper layer is thin and the conductor dimensions are large. (2) For higher frequency spectrum (over 1 MHz), the effects of a two-layer soil structure are approaching that of a uniform soil since the upper layer depth becomes large in comparison to the wavelength. (3) The results show that the quasi-static image model may be used in practical lightning studies for impulses with lower frequency content. The conditions should depend on the parameters of both layers, and the dimensions of the grounding system. (4) Larger differences between the exact and the quasi-static image model has been experienced when: (a) the upper layer is very thin, (b) the conductor length is of the same order of the upper layer wavelength (optionally $\lambda_1/3 \sim 3\lambda_1$), (c) the reflection factor is negative or positive and approaches ± 1. (5) The model is also applicable for analysis of more complex grounding system geometry.

References

[1] A. Banos, Dipole Radiation in the Presence of a Conducting Half-Space, Pergamon Press, Oxford, 1966.

[2] L.M. Brekhovskish, Waves in Layered Media, Academic Press, New York, 1960.

[3] G.J. Burke, E.K. Miller, Modeling antennas near to and penetrating a Lossy interface, IEEE Trans. Antennas Propagat. 32 (1984) 1040–1049.

[4] J.L. del Alamo, A comparison among eight different techniques to achieve an optimum estimation of electrical grounding parameters in two-layered earth, IEEE Trans. Power Delivery 8 (1993) 1890–1899.

[5] G. Dural, M. Aksun, Closed-form Green's functions for general sources and stratified media, IEEE Trans. Antennas Propagat. 43 (1995) 1545–1552.

[6] L. Grcev, Computation of transient voltages near complex grounding systems caused by lightning currents, in: Proceedings of the IEEE International Symposium on Electromagnetic Compatibility, Anaheim, CA, 1992, pp. 393–399.

[7] L. Grcev, Computer analysis of transient voltages in large grounding systems, IEEE Trans. Power Delivery 11 (1996) 815–823.

[8] L. Grcev, V. Arnautovski, Computer model for electromagnetic transients in thin wire structures above, below and penetrating the earth, in: Symposium record, Fifth International Symposium on Electric and Magnetic Fields EMF2000, Ghent, Belgium, 2000.

[9] L. Grcev, F. Dawalibi, An electromagnetic model for transients in grounding systems, IEEE Trans. Power Delivery 5 (1990) 1773–1781.

[10] R.F. Harrington, Field Computation by Moment Method, IEEE Press, New York, 1993.
[11] K. Michalski, D. Zheng, Electromagnetic scattering and radiation by surfaces of arbitrary shape in layered media, Part I: theory, IEEE Trans. Antennas Propagat. 38 (1990) 335–344.
[12] J.R. Mosig, F.E. Gardiol, A dynamic model for microstrip structures, in: P.W. Hawkes (Ed.), Advances in Electronics and Electron Physics, New York, 1982, pp. 139–237.
[13] R. Olsen, M.C. Willis, A comparison of exact and quasi-static methods for evaluating grounding systems at high frequencies, IEEE Trans. Power Delivery 11 (1996) 1071–1081.
[14] E.D. Sunde, Earth Conduction Effects in Transmission Systems, van Nostrand, New York, 1949.
[15] G.F. Tagg, Earth Resistances, George Newnes Ltd., London, 1964.
[16] T. Takashima, T. Nakae, R. Ishibashi, High frequency characteristics of impedances to ground and field distributions of ground electrodes, IEEE Trans. Power Apparatus Syst. 100 (1980) 1893–1900.
[17] F.M. Tesche, M.V. Ianoz, T. Karlsson, EMC Analysis Methods and Computational Models, Wiley, New York, 1997.
[18] F.M. Tesche, B.A. Renz, R.M. Hayes, R.G. Olsen, Development and use of a multiconductor line model for PLC assessments, in: Proceedings of the International Zurich Symposium on Electromagnetic Compatibility, Zurich, 2003, pp. 99–104.
[19] J.M. Nahman, Digital calculation of earthing systems in nonuniform soil, Archiv. Electrotechnik 62 (1980) 19–24.